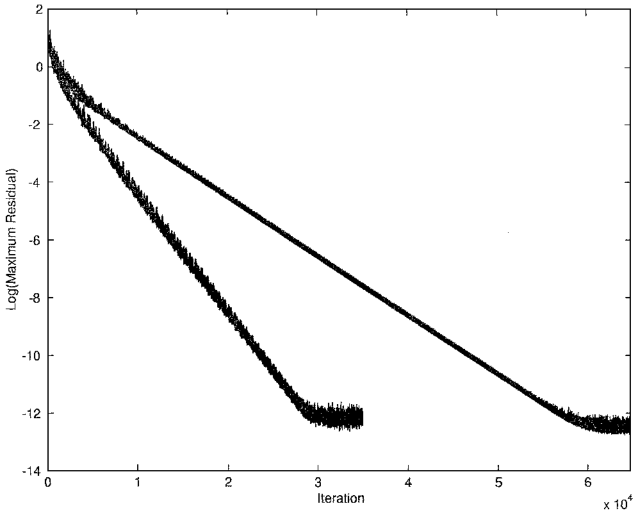

Fig. 3 Convergence histories.

the number of iterations, a significant reduction in computational work.

V. Conclusions

With this work we have presented several new ways to accelerate the convergence of an inverse design technique for constructing transonic turbomachinery cascades.

By describing a blade geometry as a mean camberline with a specified thickness distribution, we have shown how this camberline can be obtained from a Lagrangian analysis that overlays the blade onto a material line that convects from inflow to outflow. Numerical results were presented to illustrate the enhanced convergence acceleration and flow resolution that can be produced by this new approach.

We also showed how a passage-averaged flow turning distribution can be used to derive an unsteady pressure boundary condition to further accelerate our calculations to a steady state.

Acknowledgments

We are grateful to the Natural Sciences and Engineering Research Council of Canada (NSERC) for supporting this work under NSERC Grant OGP 170377. It is with pleasure that we acknowledge the numerous conversations held throughout the course of this work with T. Q. Dang and acknowledge his inverse design code on which our work is based.

References

[1]Hawthorne, W. R., Wang, C., Tan, C. S., and McCune, J. E., "Theory of Blade Design for Large Deflections, Part 1: Two-Dimensional Cascades," *Journal of Engineering for Gas Turbines and Power*, Vol. 106, No. 2, 1984, pp. 346–353.

[2]Tan, C. S., Hawthorne, W. R., McCune, J. E., and Wang, C., "Theory of Blade Design for Large Deflections, Part II: Two-Dimensional Cascades," *Journal of Engineering for Gas Turbines and Power*, Vol. 106, No. 2, 1984, pp. 354–365.

[3]Dang, T. Q., "Inverse Method for Turbomachine Blades Using Shock-Capturing Techniques," AIAA Paper 95-2465, 1995.

[4]Dang, T., and Isgro, V., "Euler-Based Inverse Method for Turbomachine Blades Part 1: Two-Dimensional Cascades," *AIAA Journal*, Vol. 33, No. 12, 1995, pp. 2309–2315.

[5]Dang, T. Q., Nerurkar, A. C., and Reddy, D. R., "Design Modification of Rotor 67 by 3D Inverse Method-Inviscid Flow Limit," American Society of Mechanical Engineers, Paper 97-GT-484, 1997.

[6]Jameson, A., Schmidt, W., and Turkel, E., "Numerical Solutions of the Euler Equations by Finite Volume Methods Using Runge–Kutta Time-Stepping Schemes," AIAA Paper 81-1259, 1981.

A. Plotkin
Associate Editor

Studies on Polygonal Slot Jets

K. Srinivasan*
Indian Institute of Technology, Guwahati 781 001, India
and
E. Rathakrishnan†
Indian Institute of Technology, Kanpur 208 016, India

Introduction

JET mixing finds application in a variety of flow systems such as combustion chambers, high-pressure valves, propulsive systems, etc. Jet mixing problems assume higher dimensions at high speeds due to compressibility effects and the presence of shocks. Passive control mechanisms have been attractive in effectively dealing with these problems. In this regard, noncircular jets are promising due to their efficacy in mixing and noise suppression. Among the noncircular jets, polygonal jets combine the advantage of streamwise vortices generated at the sharp corners and the large-scale structures rolling up from the flat surfaces. Such a combination is attractive because high-performance combustors and propulsive systems require both large-scale and fine-scale mixing. Many investigators have studied triangular jets[1–3] and rectangular jets[4–10] from different points of view. However, polygonal jets with more than four sharp corners have not been studied exhaustively. There are, however, studies on certain complex polygonal shapes such as cruciform configurations available in the literature.[11,12]

In this Note, flow characteristics of jets from polygonal slots have been investigated. Four regular polygonal slots (triangular, square, pentagonal, and hexagonal) are considered. The equivalent diameter D_e (diameter of a circle having the same area) of the slots is 10 mm. Jet issuing from slots made on thin plates are used, rather than contoured nozzles, to ensure azimuthal uniformity in the boundary-layer growth to enable a proper comparison of different geometries.[13] Furthermore, in some practical applications, expeditious manufacturing and ease of installation may dictate the use of sharp-edged slots in preference to nozzles with contoured upstream shaping.[12,14]

Details of Experiments

The experiments were carried out at the high-speed jet test facility, shown schematically in Fig. 1, of the Indian Institute of Technology, Kanpur. Different exit Mach numbers are achieved by varying the settling chamber (stagnation) pressure P_0. Circular plates of 1.5-mm thickness, over which slots of required geometry were made, were attached to the disk holder. The area ratio between the slot holder pipe and the slot was 100. The slots were flat (square) edged. The flattened edges of the slots were uniformly smooth. The centroid of the slot was chosen to be the origin in the present study (see Fig. 1).

Tests were conducted on jets issuing at several subsonic Mach numbers M_j ranging from 0.2 to 1.0 to obtain the flow characteristics. The pitot pressure was used to obtain the velocities using the isentropic relation

$$M_j = \sqrt{5\left[(P_a/P_t)^{-0.2857} - 1\right]} \tag{1}$$

where P_t and P_a are the pitot and ambient pressures, respectively. From the velocity profiles, half widths $Y_{0.5}$ and $Z_{0.5}$ were calculated. The pitot pressures were measured using a probe of 0.6-mm outer diameter and 0.4-mm inner diameter, designed according to recommendations by Nagai.[15] The flowfield was captured by pitot probe survey using a three-way traversing system. The pitot probe was connected to a PSI 9010 multichannel pressure transducer in

Received 27 September 1999; presented as Paper 2000-0613 at the AIAA 38th Aerospace Sciences Meeting, Reno, NV, 10–13 January 2000; revision received 4 April 2000; accepted for publication 11 May 2000.

*Assistant Professor, Department of Mechanical Engineering.

†Professor, Department of Aerospace Engineering.

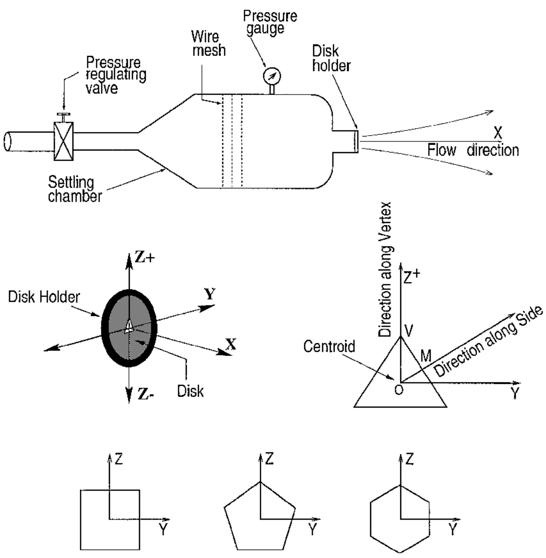

Fig. 1 Experimental setup and coordinate system.

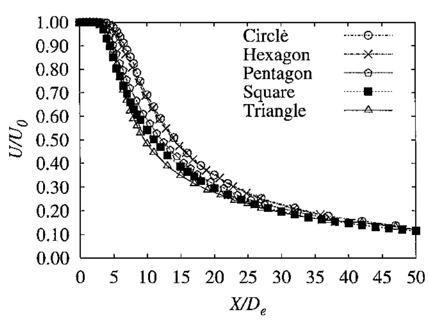

Fig. 2 Centerline velocity decay of polygonal jets at $M_j = 1.0$.

conjunction with a mercury manometer. The distance between the slot axis and the floor was kept sufficiently large to ignore the wall effects.

The uncertainty estimates were arrived at according to the method of Kline and McClintock[16] at 20:1 odds. The stagnation pressure was maintained with an accuracy of $\pm 1.7\%$, whereas the pitot pressure reading across the jet was within $\pm 0.6\%$. The uncertainty in Mach number was $\pm 3.5\%$. The uncertainty in the slot diameter was $\pm 1.2\%$, and that of the dimensionless axial distance X/D_e was ± 0.01. Throughout the experiments, the temperature varied within $\pm 1°C$.

Results and Discussion

The decay of centerline velocity U nondimensionalized by the exit velocity U_0 of various polygons are shown in Fig. 2 for Mach number 1.0. Figure 2 shows that lower-order polygons exhibit better near-field decay compared to the higher-order ones. Also, all of the polygons show better decay than the circular jet. A linear regression analysis was conducted in the range $10 \leq X/D_e \leq 30$ for the centerline decay behavior at Mach 1.0 using

$$U_0/U_c = K_u(X/D_e + C_u) \tag{2}$$

The values of mean streamwise velocity decay rate K_u and kinematic virtual origin C_u obtained are given in Table 1. With exception of the triangular jet, the value of K_u keeps decreasing as the order of the polygon increases. The kinematic virtual origins of the polygons (except the hexagon) are located upstream of the slot exit plane. The kinematic virtual origin moves downstream with increase in the order of the polygon. Note that the kinematic virtual origin of a circular jet lies downstream of the slot exit plane.[17] Thus, as circularity is approached (hexagon), the sign of C_u changes, indicating the shift of the kinematic virtual origin downstream of the slot exit plane.

Table 1 Coefficients obtained by linear regression, for centerline behavior of triangular jets at Mach number 1.0

Polygon	K_u	C_u
Triangle	0.1532	3.6432
Square	0.1612	1.1788
Pentagon	0.1548	0.7193
Hexagon	0.1496	−0.6017

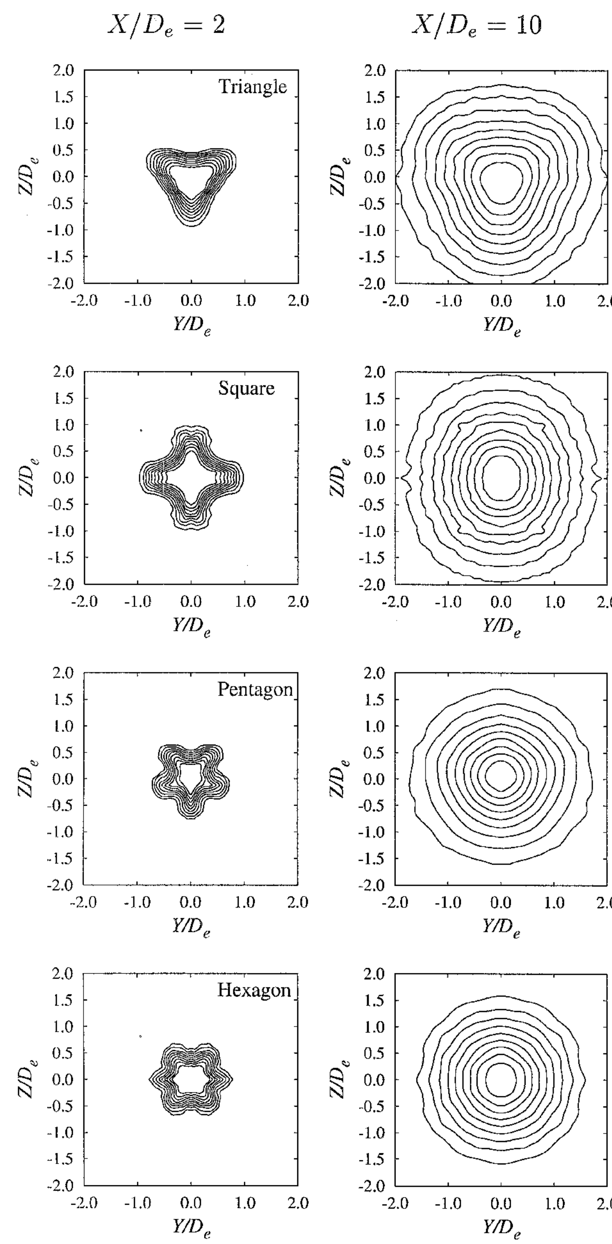

Fig. 3 Contours of constant velocity showing cross-sectional structure of polygonal jets operating at Mach number 0.4: outermost contour $0.1U_c$ and innermost contour $0.9U_c$, in steps of $0.1U_c$.

The structure of the flow at each cross section is obtained in the form of contours of constant velocity. In these contours, the local centerline velocity U_c has been chosen as the nondimensionalizing velocity. In this Note, side plane denotes the half-plane containing the midpoint of a side and the centerline (plane containing line OM in Fig. 1). The cross-sectional structures of the polygonal jets are given in Fig. 3 for Mach 0.4. Close to the exit, the cross sections of the jets were the same as that of the slot (not shown in Fig. 3). The cross section of the jets become inverted at a distance of 2 diameters. This is due to the inhibition of spread by the streamwise vortices generated at the sharp corners of the polygon (see half-width

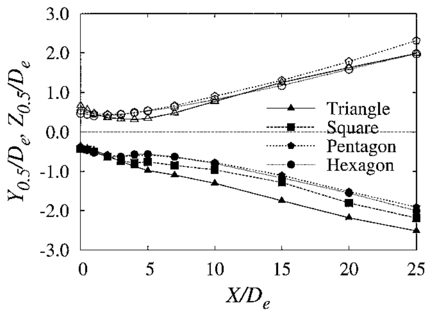

Fig. 4 Variation of half-velocity widths along vertex and side planes for polygonal jets at Mach number 1.0: solid symbols, side planes, and open symbols, vertex planes.

variation along the vertex plane in Fig. 4). Spread is maximum at locations corresponding to the midpoint of a flat side, clearly indicating the action of the large-scale structures rolling up from the flat edges. Also notice that this increased spread along the flat side direction is more pronounced in lower-order polygons. Because for polygons of equal area the length of a side of a lower-order polygon is higher than that of a higher-order polygon, it may be concluded that the length of a flat side determines the amount of spread. The area enclosed by the outermost contour ($0.1U_c$) may be taken as a measure of the size of the jet at a particular location. It is seen that the size of the lower-order polygons are larger than those of higher orders.

The half-width growths of the polygonal jets are compared in Fig. 4 for Mach number 1.0. An initial decrease in half width along the vertex planes can be seen from this plot. Observe that the hexagon, being closer to the circle, attains axisymmetry more quickly, compared to the rest of the polygons. This tendency decreases with decrease in the number of sides of the polygon. Thus, the triangular jet shows a lot of variation in its spread along vertex and side planes. The spread along side and vertex planes are different, even at 25 diameters, for triangular and pentagonal jets.

Summary

In polygonal jets, mixing processes continue to be active even in the far field. These results indicate that polygonal jets, particularly those of lower orders, may be favorably considered for use in mixing and propulsive systems.

References

[1]Koshigoe, S., Gutmark, E., Schadow, K. C., and Tubis, A., "Wave Structures in Jets of Arbitrary Shape. iii. Triangular Jets," *Physics of Fluids*, Vol. 31, No. 6, 1988, pp. 1410–1419.

[2]Quinn, W. R., "Mean Flow and Turbulence Measurements in a Triangular Turbulent Free Jet," *International Journal of Heat and Fluid Flow*, Vol. 11, No. 3, 1990, pp. 220–224.

[3]Gutmark, E., Schadow, K. C., and Wilson, K. J., "Subsonic and Supersonic Combustion Using Noncircular Injectors," *Journal of Propulsion and Power*, Vol. 7, No. 2, 1991, pp. 240–249.

[4]Van der Hegge Zijnen, B. G., "Measurements of the Velocity Distribution in a Plane Turbulent Jet of Air," *Applied Scientific Research*, Vol. A7, 1958, pp. 256–276.

[5]Marsters, G. F., "Spanwise Velocity Distributions in Jets from Rectangular Slots," *AIAA Journal*, Vol. 19, No. 2, 1981, pp. 148–152.

[6]Krothapalli, A., Hsia, Y., Baganoff, D., and Karamcheti, K., "The Role of Screech Tones in Mixing of an Underexpanded Rectangular Jet," *Journal of Sound and Vibration*, Vol. 106, No. 1, 1986, pp. 119–143.

[7]Tsuchiya, Y., Horikoshi, C., and Sato, T., "On the Spread of Rectangular Jets," *Experiments in Fluids*, Vol. 4, 1986, pp. 197–204.

[8]Tam, C. K. W., and Thies, A., "Instability of Rectangular Jets," *Journal of Fluid Mechanics*, Vol. 248, 1993, pp. 425–448.

[9]Quinn, W. R., "Streamwise Evolution of a Square Jet Cross Section," *AIAA Journal*, Vol. 30, No. 12, 1992, pp. 2852–2857.

[10]Raman, G., and Taghavi, R., "Resonant Interaction of a Linear Array of Supersonic Rectangular Jets: An Experimental Study," AIAA Paper 95-0510, 1995.

[11]Fujita, S., Osaka, H., and Ueno, G., "Three-Dimensional Jet Issuing from the Cruciform Nozzle," *Bulletin of the Japan Society of Mechanical Engineering*, Vol. 28, No. 240, 1985, pp. 1062–1068.

[12]Quinn, W. R., and Marsters, G. F., "Upstream Influence on Turbulent Jet from Cruciform Nozzles," *Aeronautical Journal*, Vol. 89, No. 882, 1985, pp. 55–58.

[13]Hussain, F., and Husain, H. S., "Elliptic Jets. Part-i: Characteristics of Unexcited and Excited Jets," *Journal of Fluid Mechanics*, Vol. 233, 1991, pp. 439–482.

[14]Gutmark, E., and Schadow, K. C., "Flow Characteristics of Orifices and Tapered Jets," *Physics of Fluids*, Vol. 30, No. 11, 1987, pp. 3448–3454.

[15]Nagai, M., "Mechanism of Pseudo-Shock Wave in Supersonic Jet," *Bulletin of the Japan Society of Mechanical Engineering*, Vol. 26, No. 212, 1983, pp. 207–214.

[16]Kline, S. J., and McClintock, F. A., "Describing Uncertainties in Single-Sample Experiments," *Mechanical Engineering*, Vol. 75, No. 1, 1953, pp. 3–8.

[17]Quinn, W. R., "On Mixing in an Elliptic Turbulent Free Jet," *Physics of Fluids A*, Vol. 1, No. 10, 1989, pp. 1716–1722.

P. J. Morris
Associate Editor

Marching Distance Functions for Smooth Control of Hyperbolic Grids

Gökhan Durmuş* and Mehmet Şerif Kavsaoğlu†
Middle East Technical University, 06531 Ankara, Turkey

Nomenclature

C = airfoil chord length
CSI = grid control parameter in ξ direction: when <1, clustering; when >1, rarefying
c = grid point chord length
i, j = grid indices, related to ξ and η directions, respectively
$\boldsymbol{i}$, $\boldsymbol{j}$ = unit vectors along x and y directions
i_ξ = i level to be controlled for grid control in ξ direction
J = Jacobian
j_η = j level to be controlled for grid control in η direction
j_ξ = j level to be controlled for grid control in ξ direction
$\boldsymbol{r}$ = position vector
s = grid spacing in η direction; marching distance
s_{j_η} = specified value of the marching distance at j_η for grid control in η direction
s_1 = initial grid spacing in η direction from the surface
s^s = exponential grid spacing function, for grid control in η direction from the surface
s^η = grid spacing function for grid control in η direction at a specified j level
V = cell volume or inverse Jacobian
x, y = Cartesian coordinates
Δi_ξ = interval of i levels for grid control in ξ direction
Δj_η = interval of j levels for grid control in η direction
Δj_ξ = interval of j levels for grid control in ξ direction
ε, ε^* = grid control parameter in η direction; ratio of the change in grid spacing to grid spacing in η direction, $\Delta s/s$
ξ, η = curvilinear coordinates

Introduction

THE hyperbolic grid generation methods have the advantages of good orthogonality, ease of clustering, and efficiency in computation time. Their fundamental principles and recent developments

Received 9 March 1999; revision received 16 November 1999; accepted for publication 21 June 2000.

*Graduate Student, Department of Aeronautical Engineering; also Research Assistant, Anadolu University Civil Aviation School, 26470 Eskişehir, Turkey.

†Associate Professor, Department of Aeronautical Engineering. Senior Member AIAA.